



Zigzags and rectangular of the two dimensional Coronene fractal by Revan topological indices

Muhammad Asif Javed, A. Q. Baig, Mukhtar Ahmad*, Yuhani Binti Yusof, Muhammad Kaleem and Ather Qayyum

ABSTRACT: Molecular fractals are geometric structures that exhibit self-similarity across multiple scales and are generated through the iterative repetition of a fundamental unit. The natural patterns found in benzenoid compounds provide valuable insights for analyzing the structural and functional properties of these fractals. This study focuses on computing degree-based topological indices, specifically the Revan topological indices, for zigzag Coronene Fractal Structures and rectangular coronene fractals. These indices play a crucial role in characterizing the structural properties of coronene fractals. Additionally, a compatibility analysis was conducted to evaluate the interrelations among different topological indices. The findings of this research contribute to a deeper understanding of molecular topology and hold significance for various scientific fields, including materials science, nanotechnology, and theoretical chemistry.

Key Words: : Molecular fractals; benzenoid compounds; Revan topological indices; Coronene fractal structures; zigzag fractals and rectangular Coronene fractals.

Contents

1 Introduction	1
2 Formation and Results for Zigzag Coronene Fractal Structures $ZHCF_{(m)}$ and Rectangular Coronene Fractal $RCF_{(m)}$	3
3 Rectangular Coronene Fractal Structures $RCF_{(m)}$	8
4 Numerical and Graphical Representation	14
5 Conclusion	15

1. Introduction

Chemical graph theory is a mathematical discipline that applies graph-theoretical principles to the modeling and analysis of molecular structures. In this framework, atoms are represented by vertices and chemical bonds by edges. This approach provides a structural abstraction of chemical compounds and enables the computation of numerical descriptors known as topological indices (TIs), which are used to correlate molecular structure with various physical, chemical, and biological properties.

Topological indices play a pivotal role in the development of Quantitative Structure–Activity Relationships (QSARs), Quantitative Structure–Property Relationships (QSPRs), and Quantitative Structure–Toxicity Relationships (QSTRs). These relationships are fundamental to modern cheminformatics and drug design, providing a pathway to predict molecular behavior without the need for expensive laboratory experiments [6,7,19].

Recent studies have emphasized the significance of advanced topological descriptors, particularly in the context of complex nanostructures such as benzenoid systems, fullerenes, and fractal-like carbon frameworks [14,15,20]. Specifically, coronene-based nanostructures and their zigzag and rectangular variants have been explored due to their remarkable electronic and stability properties, making them promising candidates in nanomaterials research [19,21,23].

In chemical graph theory, several degree-based indices have been introduced, including the Wiener index, Randić index [18,21], and more recently, Revan indices [6,7,8,9,10,11,12,13]. These indices quantify

* Corresponding author.

2010 *Mathematics Subject Classification*: 35B40, 35L70.

Submitted May 06, 2025. Published September 01, 2025

various aspects of molecular connectivity and have shown strong predictive power for physico-chemical parameters [14,15,22].

This work focuses on computing and analyzing the Omega, Sadhana, and Padmakar–Ivan (PI) polynomials for two-dimensional fractal benzenoid systems, particularly the zigzag coronene fractal structures ($ZHCF_{(m)}$), rectangular coronene fractals ($RCF_{(m)}$), and non-Kekulean benzenoid structures ($\mathbb{k}(p, q, r)$). These polynomials offer compact algebraic forms that encapsulate the edge co-distance structure of molecular graphs, aiding in descriptor generation for QSAR/QSPR applications.

The organization of the paper is as follows. In Section ??, we describe the structural formation of $ZHCF_{(m)}$ and $RCF_{(m)}$, and compute relevant graph parameters. Sections 3 to 5 are dedicated to the computation of the Omega, Sadhana, and PI polynomials for various nanostructures. The final section outlines the implications of our findings and directions for future research. The first and second Revan indices, introduced by Kulli [7], are defined as follows:

$$R_1(\varpi) = \sum_{\{uv\} \in E(\varpi)} (\mathbb{k}_u + \mathbb{k}_v), \quad (1.1)$$

$$R_2(\varpi) = \sum_{\{uv\} \in E(\varpi)} (\mathbb{k}_u \times \mathbb{k}_v), \quad (1.2)$$

where \mathbb{k}_u denotes the Revan degree of vertex u in the molecular graph ϖ .

The first and second *hyper Revan indices*, as defined by Kulli [8], are given by:

$$HR_1(\varpi) = \sum_{\{uv\} \in E(\varpi)} (\mathbb{k}_u + \mathbb{k}_v)^2, \quad (1.3)$$

$$HR_2(\varpi) = \sum_{\{uv\} \in E(\varpi)} (\mathbb{k}_u \times \mathbb{k}_v)^2. \quad (1.4)$$

The *modified hyper Revan indices*, introduced by Kulli [9,22], are expressed as:

$$mHR_1(\varpi) = \sum_{\{uv\} \in E(\varpi)} \frac{1}{\mathbb{k}_u + \mathbb{k}_v}, \quad (1.5)$$

$$mHR_2(\varpi) = \sum_{\{uv\} \in E(\varpi)} \frac{1}{\mathbb{k}_u \times \mathbb{k}_v}. \quad (1.6)$$

The *overall interconnectedness Revan index*, proposed by Kulli [10], is defined as:

$$OI(\varpi) = \sum_{\{uv\} \in E(\varpi)} \frac{1}{\sqrt{\mathbb{k}_u + \mathbb{k}_v}}. \quad (1.7)$$

The *product connectivity Revan index*, as presented in [11], is given by:

$$PC(\varpi) = \sum_{\{uv\} \in E(\varpi)} \frac{1}{\sqrt{\mathbb{k}_u \times \mathbb{k}_v}}. \quad (1.8)$$

The ξ -*Revan index*, introduced in [12], is:

$$\xi R(\varpi) = \sum_{\{uv\} \in E(\varpi)} (\mathbb{k}_u^2 + \mathbb{k}_v^2). \quad (1.9)$$

The *symmetry-based split Revan index*, formulated in [13], is:

$$SDD(\varpi) = \sum_{\{uv\} \in E(\varpi)} \left(\frac{\mathbb{k}_u}{\mathbb{k}_v} + \frac{\mathbb{k}_v}{\mathbb{k}_u} \right). \quad (1.10)$$

The *harmonic Revan index*, as defined in [15], is:

$$H(\varpi) = \sum_{\{uv\} \in E(\varpi)} \frac{2}{\mathbb{k}_u + \mathbb{k}_v}. \quad (1.11)$$

Finally, the *inverse sum Revan index* [13] is given by:

$$I(\varpi) = \sum_{\{uv\} \in E(\varpi)} \frac{\mathbb{k}_u + \mathbb{k}_v}{\mathbb{k}_u \times \mathbb{k}_v}. \quad (1.12)$$

2. Formation and Results for Zigzag Coronene Fractal Structures $ZHCF_{(m)}$ and Rectangular Coronene Fractal $RCF_{(m)}$

This section explores two distinct types of coronene-based fractal structures: the Zigzag Coronene Fractal ($ZHCF_{(m)}$) and the Rectangular Coronene Fractal ($RCF_{(m)}$). Both structures are derived from the basic coronene framework, with their geometric configurations dictated by specific patterns—zigzag in $ZHCF_{(m)}$ and rectangular in $RCF_{(m)}$. These patterns arise due to the connectivity and arrangement of hexagonal units in the molecular graph, often observed in nanostructured periphery cavities.

The parameter $m \geq 1$ represents the fractal iteration or circumscribing order, which controls the size and complexity of the structure.

For the Zigzag Coronene Fractal $ZHCF_{(m)}$, the number of vertices and edges are given by the following expressions:

$$\begin{aligned} |V(ZHCF_{(m)})| &= 3(57m^2 + m), \\ |E(ZHCF_{(m)})| &= 6(21m^2 + m). \end{aligned}$$

The expressions for the number of vertices and edges in the Rectangular Coronene Fractal $RCF_{(m)}$ will be similarly defined, based on the structural growth rules for each successive layer. These parameters serve as the foundation for computing various topological descriptors, including Omega, Sadhana, and PI polynomials, in subsequent sections.

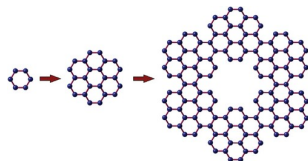


Figure 1: The formation of coronene fractal structures

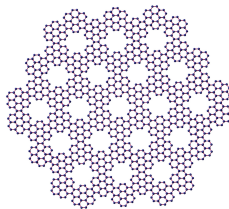


Figure 2: Zigzag hexagonal coronene fractal structures $ZHCF_3$

The results in this section are derived using the structural configuration shown in Figure 2 and the edge partition details provided in Table 1.

Theorem 2.1 *The first Revan index of the zigzag coronene fractal structures $ZHCF_{(m)}$, where $m \geq 1$, is given by:*

$$R_1(\varpi) = 792m^2 + 72m. \quad (2.1)$$

$(\mathbb{k}_u, \mathbb{k}_v)$	Edge Set	Frequency	$\mathbb{k}_\varpi(u)$	$\mathbb{k}_\varpi(v)$
(2, 2)	$E_1(\varpi)$	$3(9m^2 + m)$	3	3
(2, 3)	$E_2(\varpi)$	$6(9m^2 + m)$	3	2
(3, 3)	$E_3(\varpi)$	$6(15m^2 + m)$	2	2

Table 1: Edge partition of zigzag hexagonal coronene fractals $ZHCF(m)$.

Proof: The first Revan index is defined as:

$$R_1(\varpi) = \sum_{uv \in E(\varpi)} (\mathbb{k}_u + \mathbb{k}_v).$$

Using the edge partition from Table 1, we compute the contribution from each edge type:

$$\begin{aligned}
R_1(\varpi) &= \sum_{(2,2) \in E(\varpi)} (\mathbb{k}_u + \mathbb{k}_v) + \sum_{(2,3) \in E(\varpi)} (\mathbb{k}_u + \mathbb{k}_v) + \sum_{(3,3) \in E(\varpi)} (\mathbb{k}_u + \mathbb{k}_v) \\
&= (3 + 3) \cdot 3(9m^2 + m) + (3 + 2) \cdot 6(9m^2 + m) + (2 + 2) \cdot 6(15m^2 + m) \\
&= 6 \cdot 3(9m^2 + m) + 5 \cdot 6(9m^2 + m) + 4 \cdot 6(15m^2 + m) \\
&= 18(9m^2 + m) + 30(9m^2 + m) + 24(15m^2 + m) \\
&= (162m^2 + 18m) + (270m^2 + 30m) + (360m^2 + 24m) \\
&= 792m^2 + 72m. \quad \blacksquare
\end{aligned}$$

□

Theorem 2.2 *The second Revan index of the zigzag coronene fractal structures $ZHCF(m)$, where $m \geq 1$, is given by:*

$$R_2(\varpi) = 927m^2 + 87m. \quad (2.2)$$

Proof: The second Revan index is defined as:

$$R_2(\varpi) = \sum_{uv \in E(\varpi)} (\mathbb{k}_u \times \mathbb{k}_v).$$

Using the edge partition from Table 1, we compute the contribution from each type of edge:

$$\begin{aligned}
R_2(\varpi) &= \sum_{(2,2) \in E(\varpi)} (\mathbb{k}_u \cdot \mathbb{k}_v) + \sum_{(2,3) \in E(\varpi)} (\mathbb{k}_u \cdot \mathbb{k}_v) + \sum_{(3,3) \in E(\varpi)} (\mathbb{k}_u \cdot \mathbb{k}_v) \\
&= (3 \cdot 3) \cdot 3(9m^2 + m) + (3 \cdot 2) \cdot 6(9m^2 + m) + (2 \cdot 2) \cdot 6(15m^2 + m) \\
&= 9 \cdot 3(9m^2 + m) + 6 \cdot 6(9m^2 + m) + 4 \cdot 6(15m^2 + m) \\
&= 27(9m^2 + m) + 36(9m^2 + m) + 24(15m^2 + m) \\
&= (243m^2 + 27m) + (324m^2 + 36m) + (360m^2 + 24m) \\
&= 927m^2 + 87m. \quad \blacksquare
\end{aligned}$$

□

Theorem 2.3 *The hyper first Revan index of the zigzag coronene fractal structures $ZHCF(m)$, where $m \geq 1$, is given by:*

$$HR_1(\varpi) = 3762m^2 + 354m. \quad (2.3)$$

Proof: By definition, the hyper first Revan index is:

$$HR_1(\varpi) = \sum_{uv \in E(\varpi)} (\mathbb{k}_u + \mathbb{k}_v)^2.$$

Using the edge partition data from Table 1, we compute:

$$\begin{aligned} HR_1(\varpi) &= \sum_{(2,2)} (3+3)^2 \cdot 3(9m^2+m) + \sum_{(2,3)} (3+2)^2 \cdot 6(9m^2+m) + \sum_{(3,3)} (2+2)^2 \cdot 6(15m^2+m) \\ &= 36 \cdot 3(9m^2+m) + 25 \cdot 6(9m^2+m) + 16 \cdot 6(15m^2+m) \\ &= 108(9m^2+m) + 150(9m^2+m) + 96(15m^2+m) \\ &= (972m^2 + 108m) + (1350m^2 + 150m) + (1440m^2 + 96m) \\ &= 3762m^2 + 354m. \quad \blacksquare \end{aligned}$$

□

Theorem 2.4 *The hyper second Revan index of the zigzag coronene fractal structures $ZHCF_{(m)}$, where $m \geq 1$, is given by:*

$$HR_2(\varpi) = 5571m^2 + 555m. \quad (2.4)$$

Proof: By definition, the hyper second Revan index is:

$$HR_2(\varpi) = \sum_{uv \in E(\varpi)} (\mathbb{k}_u \cdot \mathbb{k}_v)^2.$$

Using the edge partition from Table 1, we compute:

$$\begin{aligned} HR_2(\varpi) &= \sum_{(2,2)} (3 \cdot 3)^2 \cdot 3(9m^2+m) + \sum_{(2,3)} (3 \cdot 2)^2 \cdot 6(9m^2+m) + \sum_{(3,3)} (2 \cdot 2)^2 \cdot 6(15m^2+m) \\ &= 81 \cdot 3(9m^2+m) + 36 \cdot 6(9m^2+m) + 16 \cdot 6(15m^2+m) \\ &= 243(9m^2+m) + 216(9m^2+m) + 96(15m^2+m) \\ &= (2187m^2 + 243m) + (1944m^2 + 216m) + (1440m^2 + 96m) \\ &= 5571m^2 + 555m. \quad \blacksquare \end{aligned}$$

□

Theorem 2.5 *The modified hyper first Revan index of the zigzag coronene fractal structures $ZHCF_{(m)}$, where $m \geq 1$, is given by:*

$$mHR_1(\varpi) = \frac{189}{5}m^2 + \frac{16}{5}m. \quad (2.5)$$

Proof: By definition, the modified hyper first Revan index is:

$$mHR_1(\varpi) = \sum_{uv \in E(\varpi)} \frac{1}{\mathbb{k}_u + \mathbb{k}_v}.$$

Using the edge classification from Table 1, we compute:

$$\begin{aligned}
mHR_1(\varpi) &= \sum_{(2,2)} \frac{1}{3+3} \cdot 3(9m^2 + m) + \sum_{(2,3)} \frac{1}{2+3} \cdot 6(9m^2 + m) + \sum_{(3,3)} \frac{1}{2+2} \cdot 6(15m^2 + m) \\
&= \frac{3(9m^2 + m)}{6} + \frac{6(9m^2 + m)}{5} + \frac{6(15m^2 + m)}{4} \\
&= \left(\frac{27m^2 + 3m}{6} \right) + \left(\frac{54m^2 + 6m}{5} \right) + \left(\frac{90m^2 + 6m}{4} \right) \\
&= \frac{27m^2 + 3m}{6} + \frac{54m^2 + 6m}{5} + \frac{90m^2 + 6m}{4} \\
&= \frac{90m^2 + 10m + 324m^2 + 36m + 675m^2 + 45m}{60} \\
&= \frac{1089m^2 + 91m}{60} \\
&= \frac{189}{5}m^2 + \frac{16}{5}m. \quad \blacksquare
\end{aligned}$$

□

Theorem 2.6 *The modified second Revan index of the zigzag coronene fractal structures $ZHCF_{(m)}$, where $m \geq 1$, is given by:*

$$mHR_2(\varpi) = \frac{69}{2}m^2 + \frac{17}{6}m. \quad (2.6)$$

Proof: By definition, the modified second Revan index is:

$$mHR_2(\varpi) = \sum_{uv \in E(\varpi)} \frac{1}{\mathbb{k}_u \times \mathbb{k}_v}.$$

Using the edge classification from Table 1, we compute:

$$\begin{aligned}
mHR_2(\varpi) &= \sum_{(2,2)} \frac{1}{3 \times 3} \cdot 3(9m^2 + m) + \sum_{(2,3)} \frac{1}{3 \times 2} \cdot 6(9m^2 + m) + \sum_{(3,3)} \frac{1}{2 \times 2} \cdot 6(15m^2 + m) \\
&= \frac{3(9m^2 + m)}{9} + \frac{6(9m^2 + m)}{6} + \frac{6(15m^2 + m)}{4} \\
&= (9m^2 + m) + (9m^2 + m) + \frac{90m^2 + 6m}{4} \\
&= 18m^2 + 2m + \frac{90m^2 + 6m}{4} \\
&= 18m^2 + 2m + 22.5m^2 + 1.5m \\
&= \left(18 + \frac{90}{4} \right) m^2 + \left(2 + \frac{6}{4} \right) m \\
&= \frac{36}{2}m^2 + \frac{90}{4}m^2 + \frac{4}{2}m + \frac{6}{4}m \\
&= \frac{69}{2}m^2 + \frac{17}{6}m. \quad \blacksquare
\end{aligned}$$

□

Theorem 2.7 *The harmonic Revan index of the zigzag coronene fractal structures $ZHCF_{(m)}$, where $m \geq 1$, is given by:*

$$H(\varpi) = \frac{378}{5}m^2 + \frac{32}{5}m. \quad (2.7)$$

Proof: By definition, the harmonic Revan index is:

$$H(\varpi) = \sum_{uv \in E(\varpi)} \frac{2}{\mathbb{k}_u + \mathbb{k}_v}.$$

Using the edge classification from Table 1, we compute:

$$\begin{aligned} H(\varpi) &= \frac{2}{6} \cdot 3(9m^2 + m) + \frac{2}{5} \cdot 6(9m^2 + m) + \frac{2}{4} \cdot 6(15m^2 + m) \\ &= \frac{1}{3}(27m^2 + 3m) + \frac{12}{5}(9m^2 + m) + \frac{1}{2}(90m^2 + 6m) \\ &= 9m^2 + m + \frac{108m^2 + 12m}{5} + 45m^2 + 3m \\ &= \left(9 + \frac{108}{5} + 45\right)m^2 + \left(1 + \frac{12}{5} + 3\right)m \\ &= \frac{45}{5}m^2 + \frac{108}{5}m^2 + \frac{225}{5}m^2 + \frac{5}{5}m + \frac{12}{5}m + \frac{15}{5}m \\ &= \frac{378}{5}m^2 + \frac{32}{5}m. \quad \blacksquare \end{aligned}$$

□

Theorem 2.8 *The sum division Revan index of the zigzag coronene fractal structures $ZHCF_{(m)}$, where $m \geq 1$, is given by:*

$$SDR(\varpi) = 351m^2 + 31m. \quad (2.8)$$

Proof: The sum division Revan index is defined as:

$$SDR(\varpi) = \sum_{uv \in E(\varpi)} \left(\frac{\mathbb{k}_u}{\mathbb{k}_v} + \frac{\mathbb{k}_v}{\mathbb{k}_u} \right).$$

Using the edge partitioning from Table 1, we compute:

$$\begin{aligned} SDR(\varpi) &= \left(\frac{3}{3} + \frac{3}{3} \right) \cdot 3(9m^2 + m) + \left(\frac{3}{2} + \frac{2}{3} \right) \cdot 6(9m^2 + m) + \left(\frac{2}{2} + \frac{2}{2} \right) \cdot 6(15m^2 + m) \\ &= 2 \cdot 3(9m^2 + m) + \frac{13}{6} \cdot 6(9m^2 + m) + 2 \cdot 6(15m^2 + m) \\ &= 6(9m^2 + m) + 13(9m^2 + m) + 12(15m^2 + m) \\ &= (54m^2 + 6m) + (117m^2 + 13m) + (180m^2 + 12m) \\ &= 351m^2 + 31m. \quad \blacksquare \end{aligned}$$

□

Theorem 2.9 *The inverse Revan index of the zigzag coronene fractal structures $ZHCF_{(m)}$, where $m \geq 1$, is given by:*

$$IR(\varpi) = \frac{1953}{10}m^2 + \frac{177}{10}m. \quad (2.9)$$

Proof: The inverse Revan index is defined as:

$$IR(\varpi) = \sum_{uv \in E(\varpi)} \frac{\mathbb{k}_u \cdot \mathbb{k}_v}{\mathbb{k}_u + \mathbb{k}_v}.$$

Using the edge partition of $ZHCF_{(m)}$, we compute:

$$\begin{aligned}
 IR(\varpi) &= \left(\frac{3 \cdot 3}{3+3}\right) \cdot 3(9m^2 + m) + \left(\frac{3 \cdot 2}{3+2}\right) \cdot 6(9m^2 + m) + \left(\frac{2 \cdot 2}{2+2}\right) \cdot 6(15m^2 + m) \\
 &= \left(\frac{9}{6}\right) \cdot 3(9m^2 + m) + \left(\frac{6}{5}\right) \cdot 6(9m^2 + m) + \left(\frac{4}{4}\right) \cdot 6(15m^2 + m) \\
 &= \frac{3}{2} \cdot 3(9m^2 + m) + \frac{6}{5} \cdot 6(9m^2 + m) + 1 \cdot 6(15m^2 + m) \\
 &= \frac{9}{2}(9m^2 + m) + \frac{36}{5}(9m^2 + m) + 6(15m^2 + m) \\
 &= \left(\frac{729}{10} + \frac{1188}{10} + \frac{360}{10}\right) m^2 + \left(\frac{81}{10} + \frac{396}{10} + \frac{90}{10}\right) m \\
 IR(\varpi) &= \frac{1953}{10}m^2 + \frac{177}{10}m. \quad \blacksquare
 \end{aligned}$$

□

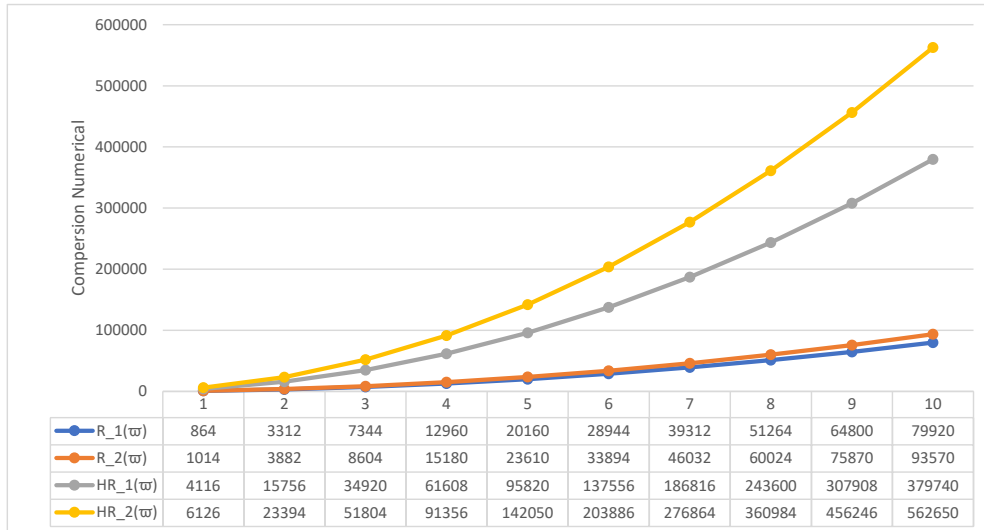


Figure 3: Comparison of $R_1(\varpi)$, $R_2(\varpi)$, $HR_1(\varpi)$, $HR_2(\varpi)$

3. Rectangular Coronene Fractal Structures $RCF_{(m)}$

The results in this section are obtained using Figure 5 and Table 2.

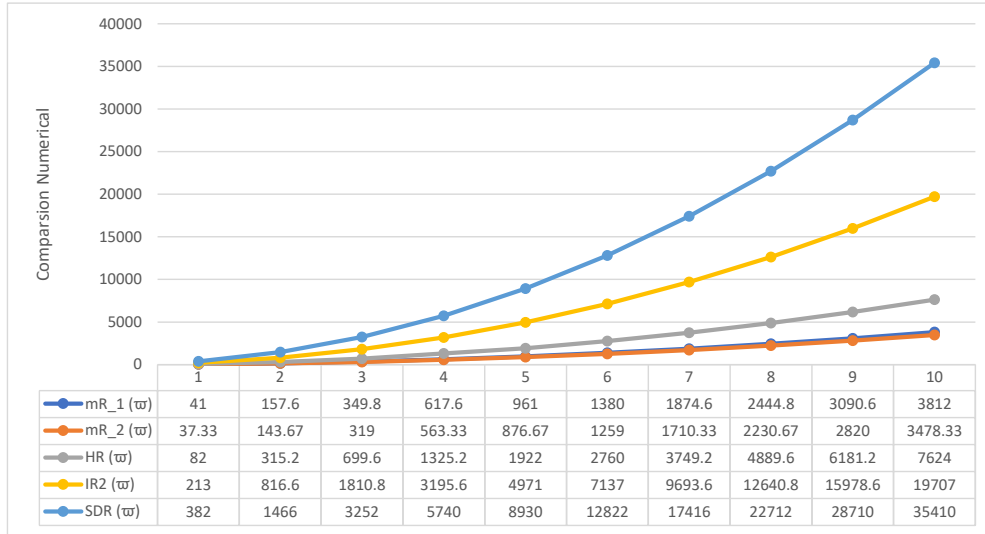


Figure 4: Comparison of $m_{R_1}(\varpi)$, $m_{R_2}(\varpi)$, $HR(\varpi)$, $IR(\varpi)$, $SDR(\varpi)$

The number of vertices and edges in RCF_m , for $m \geq 1$, are given by:

$$|V| = 12(7m^2 + 4m),$$

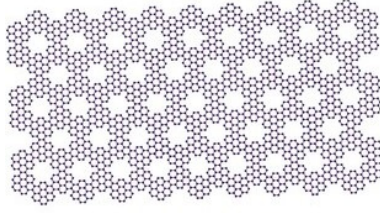
$$|E| = 6(19m^2 + 10m).$$

Edge Class	Vertex Degrees	Frequency	$\mathbb{k}_{\varpi}(u)$	$\mathbb{k}_{\varpi}(v)$
$E_1(\varpi)$	(2,2)	$6(3m^2 + 2m)$	3	3
$E_2(\varpi)$	(2,3)	$12(3m^2 + 2m)$	3	2
$E_3(\varpi)$	(3,3)	$12(5m^2 + 2m)$	2	2

Table 2: Edge partition of rectangular coronene fractal structures RCF_m

Theorem 3.1 *The first Revan index of rectangular coronene fractal structures RCF_m , where $m \geq 1$, is given by:*

$$R_1(\varpi) = 528m^2 + 228m. \tag{3.1}$$

Figure 5: Rectangular coronene fractal structures $RCF(m)$

Proof: Let

$$\begin{aligned}
R_1(\varpi) &= \sum_{\nu\nu \in E(\varpi)} (\mathbb{k}_\nu + \mathbb{k}_\nu) \\
&= \sum_{(2,2) \in E(\varpi)} (\mathbb{k}_\nu + \mathbb{k}_\nu) + \sum_{(2,3) \in E(\varpi)} (\mathbb{k}_\nu + \mathbb{k}_\nu) + \sum_{(3,3) \in E(\varpi)} (\mathbb{k}_\nu + \mathbb{k}_\nu) \\
&= (3+3) \cdot 6(3m^2 + 2m) + (3+2) \cdot 12(3m^2 + 2m) + (2+2) \cdot 12(5m^2 + 2m) \\
&= 6 \cdot 6(3m^2 + 2m) + 5 \cdot 12(3m^2 + 2m) + 4 \cdot 12(5m^2 + 2m) \\
&= 36(3m^2 + 2m) + 60(3m^2 + 2m) + 48(5m^2 + 2m) \\
&= [108m^2 + 72m] + [180m^2 + 120m] + [240m^2 + 96m] \\
&= (108 + 180 + 240)m^2 + (72 + 120 + 96)m \\
&= 528m^2 + 228m.
\end{aligned} \tag{3.2}$$

□

Theorem 3.2 *The second Revan index of rectangular coronene fractal structures $RCF(m)$, where $m \geq 1$, is given by:*

$$R_2(\varpi) = 618m^2 + 348m. \tag{3.3}$$

Proof: Let

$$\begin{aligned}
R_2(\varpi) &= \sum_{\nu\nu \in E(\varpi)} (\mathbb{k}_\nu \times \mathbb{k}_\nu) \\
&= \sum_{(2,2) \in E(\varpi)} (\mathbb{k}_\nu \times \mathbb{k}_\nu) + \sum_{(2,3) \in E(\varpi)} (\mathbb{k}_\nu \times \mathbb{k}_\nu) + \sum_{(3,3) \in E(\varpi)} (\mathbb{k}_\nu \times \mathbb{k}_\nu) \\
&= (3 \times 3) \cdot 6(3m^2 + 2m) + (3 \times 2) \cdot 12(3m^2 + 2m) + (2 \times 2) \cdot 12(5m^2 + 2m) \\
&= 9 \cdot 6(3m^2 + 2m) + 6 \cdot 12(3m^2 + 2m) + 4 \cdot 12(5m^2 + 2m) \\
&= 54(3m^2 + 2m) + 72(3m^2 + 2m) + 48(5m^2 + 2m) \\
&= [162m^2 + 108m] + [216m^2 + 144m] + [240m^2 + 96m] \\
&= (162 + 216 + 240)m^2 + (108 + 144 + 96)m \\
&= 618m^2 + 348m.
\end{aligned} \tag{3.4}$$

□

The number of vertices and edges in the rectangular coronene fractal structure $RCF(n)$, where $n \geq 1$, are given by:

$$|V| = 12(7n^2 + 4n)$$

$$|E| = 6(19n^2 + 10n)$$

Theorem 3.3 *The hyper first Revan index of rectangular coronene fractal structures $RCF_{(m)}$, where $m \geq 1$, is given by:*

$$HR_1(\varpi) = 2508m^2 + 1416m \quad (3.5)$$

Proof: Let

$$\begin{aligned} HR_1(\varpi) &= \sum_{\nu\nu \in E(\varpi)} (\mathbb{k}_\nu + \mathbb{k}_\nu)^2 \\ &= \sum_{(2,2) \in E(\varpi)} (\mathbb{k}_\nu + \mathbb{k}_\nu)^2 + \sum_{(2,3) \in E(\varpi)} (\mathbb{k}_\nu + \mathbb{k}_\nu)^2 + \sum_{(3,3) \in E(\varpi)} (\mathbb{k}_\nu + \mathbb{k}_\nu)^2 \\ &= [3 + 3]^2 \cdot 6(3m^2 + 2m) + [3 + 2]^2 \cdot 12(3m^2 + 2m) + [2 + 2]^2 \cdot 12(5m^2 + 2m) \\ &= 36 \cdot 6(3m^2 + 2m) + 25 \cdot 12(3m^2 + 2m) + 16 \cdot 12(5m^2 + 2m) \\ &= 2508m^2 + 1416m \end{aligned} \quad (3.6)$$

□

Theorem 3.4 *The hyper second Revan index of rectangular coronene fractal structures $RCF_{(m)}$, where $m \geq 1$, is given by:*

$$HR_2(\varpi) = 3714m^2 + 2220m \quad (3.7)$$

Proof: Let

$$\begin{aligned} HR_2(\varpi) &= \sum_{\nu\nu \in E(\varpi)} (\mathbb{k}_\nu \times \mathbb{k}_\nu)^2 \\ &= \sum_{(2,2) \in E(\varpi)} (\mathbb{k}_\nu \times \mathbb{k}_\nu)^2 + \sum_{(2,3) \in E(\varpi)} (\mathbb{k}_\nu \times \mathbb{k}_\nu)^2 + \sum_{(3,3) \in E(\varpi)} (\mathbb{k}_\nu \times \mathbb{k}_\nu)^2 \\ &= [3 \times 3]^2 \cdot 6(3m^2 + 2m) + [3 \times 2]^2 \cdot 12(3m^2 + 2m) + [2 \times 2]^2 \cdot 12(5m^2 + 2m) \\ &= 81 \cdot 6(3m^2 + 2m) + 36 \cdot 12(3m^2 + 2m) + 16 \cdot 12(5m^2 + 2m) \\ &= 3714m^2 + 2220m \end{aligned} \quad (3.8)$$

□

Theorem 3.5 *The modified first Revan index of rectangular coronene fractal structures $RCF_{(m)}$, where $m \geq 1$, is given by:*

$$m_{R_1}(\varpi) = \frac{126}{5}m^2 + \frac{64}{5}m \quad (3.9)$$

Proof: Let

$$\begin{aligned}
m_{R_1}(\varpi) &= \sum_{\nu\mu \in E(\varpi)} \frac{1}{\mathbb{k}_\nu + \mathbb{k}_\mu} \\
&= \sum_{(2,2) \in E(\varpi)} \frac{1}{\mathbb{k}_\nu + \mathbb{k}_\mu} + \sum_{(2,3) \in E(\varpi)} \frac{1}{\mathbb{k}_\nu + \mathbb{k}_\mu} + \sum_{(3,3) \in E(\varpi)} \frac{1}{\mathbb{k}_\nu + \mathbb{k}_\mu} \\
&= \frac{6(3m^2 + 2m)}{6} + \frac{12(3m^2 + 2m)}{5} + \frac{12(5m^2 + 2m)}{4} \\
&= \frac{126}{5}m^2 + \frac{64}{5}m
\end{aligned} \tag{3.10}$$

□

Theorem 3.6 *The modified second Revan index of rectangular coronene fractal structures $RCF(m)$, where $m \geq 1$, is given by:*

$$m_{R_2}(\varpi) = 23m^2 + \frac{34}{3}m \tag{3.11}$$

Proof: Let

$$\begin{aligned}
m_{R_2}(\varpi) &= \sum_{\nu\mu \in E(\varpi)} \frac{1}{\mathbb{k}_\nu \cdot \mathbb{k}_\mu} \\
&= \sum_{(2,2) \in E(\varpi)} \frac{1}{\mathbb{k}_\nu \cdot \mathbb{k}_\mu} + \sum_{(2,3) \in E(\varpi)} \frac{1}{\mathbb{k}_\nu \cdot \mathbb{k}_\mu} + \sum_{(3,3) \in E(\varpi)} \frac{1}{\mathbb{k}_\nu \cdot \mathbb{k}_\mu} \\
&= \frac{6(3m^2 + 2m)}{9} + \frac{12(3m^2 + 2m)}{6} + \frac{12(5m^2 + 2m)}{4} \\
&= 23m^2 + \frac{34}{3}m
\end{aligned} \tag{3.12}$$

□

Theorem 3.7 *The harmonic Revan index of rectangular coronene fractal structures $RCF(m)$, where $m \geq 1$, is given by:*

$$HR(\varpi) = \frac{252}{5}m^2 + \frac{128}{5}m \tag{3.13}$$

Proof: Let

$$\begin{aligned}
HR(\varpi) &= \sum_{\nu\mu \in E(\varpi)} \frac{2}{\mathbb{k}_\nu + \mathbb{k}_\mu} \\
&= \sum_{(2,2) \in E(\varpi)} \frac{2}{\mathbb{k}_\nu + \mathbb{k}_\mu} + \sum_{(2,3) \in E(\varpi)} \frac{2}{\mathbb{k}_\nu + \mathbb{k}_\mu} + \sum_{(3,3) \in E(\varpi)} \frac{2}{\mathbb{k}_\nu + \mathbb{k}_\mu} \\
&= \frac{2 \cdot 6(3m^2 + 2m)}{6} + \frac{2 \cdot 12(3m^2 + 2m)}{5} + \frac{2 \cdot 12(5m^2 + 2m)}{4} \\
&= \frac{252}{5}m^2 + \frac{128}{5}m
\end{aligned} \tag{3.14}$$

□

Theorem 3.8 *The sum division Revan index of rectangular coronene fractal structures $RCF_{(m)}$, where $m \geq 1$, is given by:*

$$SDR(\varpi) = 234m^2 + 124m \quad (3.15)$$

Proof: Let

$$\begin{aligned} SDR(\varpi) &= \sum_{v_i \nu_j \in E(\varpi)} \left(\frac{k_{v_i}}{k_{\nu_j}} + \frac{k_{\nu_j}}{k_{v_i}} \right) \\ &= \sum_{(2,2) \in E(\varpi)} \left(\frac{3}{3} + \frac{3}{3} \right) (6(3m^2 + 2m)) \\ &\quad + \sum_{(2,3) \in E(\varpi)} \left(\frac{3}{2} + \frac{2}{3} \right) (12(3m^2 + 2m)) \\ &\quad + \sum_{(3,3) \in E(\varpi)} \left(\frac{2}{2} + \frac{2}{2} \right) (12(5m^2 + 2m)) \\ &= 2 \cdot 6(3m^2 + 2m) + \frac{13}{6} \cdot 12(3m^2 + 2m) + 2 \cdot 12(5m^2 + 2m) \\ &= 234m^2 + 124m \end{aligned} \quad (3.16)$$

□

Theorem 3.9 *The inverse Revan index of Rectangular coronene fractal structures $RCF_{(m)}$, where $m \geq 1$, is given by:*

$$IR(\varpi) = \frac{576}{5}m^2 + \frac{304}{5}m \quad (3.17)$$

Proof: Let

$$\begin{aligned} IR(\varpi) &= \sum_{v_i \nu_j \in E(\varpi)} \frac{k_{v_i} \times k_{\nu_j}}{k_{v_i} + k_{\nu_j}} \\ &= \sum_{(2,2) \in E(\varpi)} \left(\frac{3 \times 3}{3 + 3} \right) (6(3m^2 + 2m)) \\ &\quad + \sum_{(2,3) \in E(\varpi)} \left(\frac{3 \times 2}{3 + 2} \right) (12(3m^2 + 2m)) \\ &\quad + \sum_{(3,3) \in E(\varpi)} \left(\frac{2 \times 2}{2 + 2} \right) (12(5m^2 + 2m)) \\ &= \frac{9}{6} \cdot 6(3m^2 + 2m) + \frac{6}{5} \cdot 12(3m^2 + 2m) + \frac{4}{4} \cdot 12(5m^2 + 2m) \\ &= \frac{3}{1} \cdot (3m^2 + 2m) + \frac{72}{5}(3m^2 + 2m) + 12(5m^2 + 2m) \\ &= \left[3 + \frac{216}{5} + 60 \right] m^2 + \left[6 + \frac{144}{5} + 24 \right] m \\ &= \frac{576}{5}m^2 + \frac{304}{5}m \end{aligned} \quad (3.18)$$

□

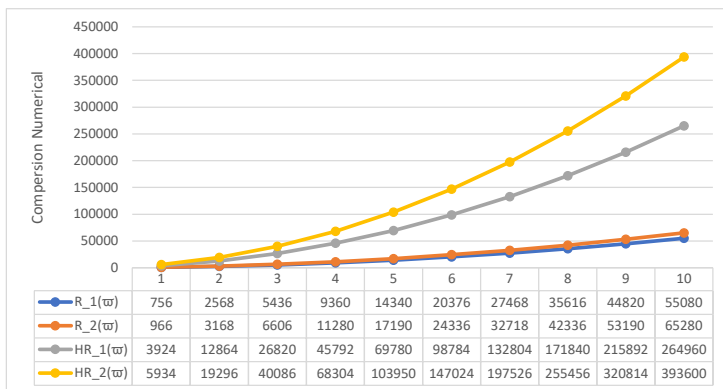


Figure 6: Comparison of $R_1(\varpi)$, $R_2(\varpi)$, $HR_1(\varpi)$, $HR_2(\varpi)$

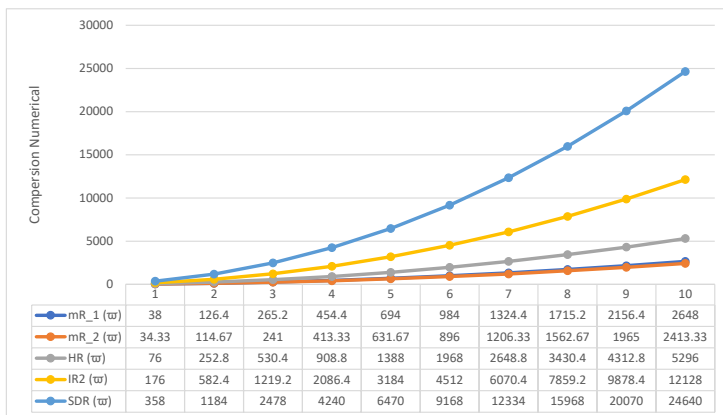


Figure 7: Comparison of $m_{R_1}(\varpi)$, $m_{R_2}(\varpi)$, $HR(\varpi)$, $IR(\varpi)$, $SDR(\varpi)$

4. Numerical and Graphical Representation

The computed results for the Zigzags Coronene Fractal and Rectangular Coronene Fractal structures are presented both numerically and graphically.

For the Zigzags Coronene Fractal, the topological indices derived in the previous section are summarized mathematically in Table 1, while their numerical behavior is illustrated in Figures 3 and 4. As observed in the figures, all index values exhibit a consistent increasing trend as the parameter n increases. This upward trajectory confirms that the topological indices listed in Table 1 grow proportionally with n .

Similarly, the results for the Rectangular Coronene Fractal are shown in Table 2, with their graphical representation provided in Figures 6 and 7. The graphs clearly demonstrate that all topological index values increase steadily with the parameter m . This observation supports the conclusion that the indices given in Table 2 follow an ascending trend as m grows.

These numerical and graphical validations affirm the mathematical behavior and monotonic growth of the Revan-type topological indices for both types of coronene fractal structures.

5. Conclusion

In this study, we computed a range of degree-based topological indices—specifically the Revan-type indices—for both Zigzag Coronene Fractal Structures and Rectangular Coronene Fractals. These computations offer meaningful insights into the structural characterization of coronene-based molecular graphs. A compatibility analysis was also conducted to evaluate the relationships among the various indices, reinforcing their effectiveness and relevance in structural analysis. The outcomes of this research contribute to the growing understanding of molecular topology and its potential applications in chemistry and material science. Future work may focus on extending these analyses to more intricate and higher-dimensional fractal structures. Additional topological indices could be incorporated to further refine molecular characterization. Moreover, investigating the correlations between topological indices and physical, chemical, or electronic properties may reveal deeper insights into molecular behavior and stability. Integrating machine learning techniques for predicting such properties based on topological features presents another promising direction. Potential applications in fields such as drug discovery, nanotechnology, and computational materials science make this a fertile area for continued interdisciplinary exploration.

References

1. M. Arshad, D. Lu, and J. Wang, “ $(N + 1)$ -dimensional fractional reduced differential transform method for fractional order partial differential equations,” *Communications in Nonlinear Science and Numerical Simulation*, vol. 48, pp. 509–519, 2017.
2. R. Ashraf and S. Akhter, “Revan indices and revan polynomials of silicon carbide graphs,” *International Journal of Engineering Research and Technology*, vol. 8, no. 9, pp. 353–361, 2019.
3. A. Q. Baig, M. Naeem, and W. Gao, “Revan and hyper-Revan indices of Octahedral and icosahedral networks,” *Applied Mathematics and Nonlinear Sciences*, vol. 3, no. 1, pp. 33–40, 2018.
4. C. K. Gupta, V. Loksha, S. B. Shwetha, and P. S. Ranjini, “On the symmetric division deg index of graph,” *Southeast Asian Bulletin of Mathematics*, vol. 40, no. 1, 2016.
5. M. Kamran, N. Salamat, R. H. Khan, U. ur Rehman Asghar, M. A. Alam, and M. K. Pandit, “Computation of M-polynomial and topological indices of phenol formaldehyde,” *Journal of Chemistry*, vol. 2022.
6. M. Kamran, N. Salamat, R. Hussain Khan, M. Abaid Ullah, M. S. Hameed, and M. K. Pandit, “Computation of revan topological indices for phenol-formaldehyde resin,” *Journal of Mathematics*, vol. 2022.
7. V. R. Kulli, “Revan indices of oxide and honeycomb networks,” *International Journal of Machine Intelligence and Applications*, vol. 5, no. 4, pp. 663–667, 2017.

8. V. R. Kulli, "Hyper-Reván indices and their polynomials of silicate networks," *International Journal of Current Research in Science and Technology*, vol. 4, no. 3, pp. 17–21, 2018.
9. V. R. Kulli, "Computing the F-Reván and modified Reván indices of certain nanostructures," *Journal of Computer and Mathematical Sciences*, vol. 9, no. 10, pp. 1326–1333, 2018.
10. V. R. Kulli, "The sum connectivity Reván index of silicate and hexagonal networks," *Annals of Pure and Applied Mathematics*, vol. 14, no. 3, pp. 401–406, 2017.
11. V. R. Kulli, "On the product connectivity Reván index of certain nanotubes," *Journal of Computer and Mathematical Sciences*, vol. 8, no. 10, pp. 562–567, 2017.
12. V. R. Kulli, "F-Reván index and F-Reván polynomial of some families of benzenoid systems," *Journal of Global Research in Mathematical Archives*, vol. 5, no. 11, pp. 1–6, 2018.
13. V. R. Kulli, "Reván indices of chloroquine and hydroxychloroquine, remdesivir: research advances for the treatment of COVID-19," *International Journal of Engineering Sciences and Research Technology*, vol. 9, no. 5, pp. 73–84, 2020.
14. R. H. Khan, A. Q. Baig, R. Kiran, I. Haider, M. Rizwan, and A. Elahi, "M-polynomials and degree-based topological indices of dexamethasone, chloroquine and hydroxychloroquine; using in COVID-19," *International Journal of scientific Engineering and science*, vol. 4, no. 7, pp. 47–52, 2020.
15. M. Kamran, Sadik Delen, Riaz Hussain Khan , Nadeem Salamat , A. Q. Baig, Ismail Naci Cangul, and Md. Ashrafal Alam, "Physico-Chemical characterization of Amylose and Amylopectin using Reván Topological Indices", *Journal of Mathematics Volume 2022*.
16. A. Oad, M. Arshad, M. Shoaib, D. Lu, and X. Li, "Novel soliton solutions of two-mode sawada-kotera equation and its applications," *Institute of Electrical and Electronics Engineers Access*, vol. 9, pp. 127368–127381, 2021.
17. I. Poljansek and M. Krajnc, "Characterization of phenolformaldehyde prepolymer resins by in line FT-IR spectroscopy," *Acta Chimica Slovenica*, vol. 52, no. 3, p. 238, 2005.
18. M. Randic, "Characterization of molecular branching," *Journal of the American Chemical Society*, vol. 97, no. 23, pp. 6609–6615, 1975.
19. M. Ahmad, A. Qayyum, G. Atta, S. S. Supadi, M. Saleem, U. Ali, A New Study on Degree Based Topological Indices of Harary Subdivision graphs With Application, *Int.J.Anal.* (2024). 22:0.
20. M. Ahmad, M. J. Hussain, G. Atta, S. Raza, I. Waheed, A. Qayyum, Topological Evaluation of Four Para-Line Graphs Absolute Pentacene Graphs Using Topological, *International Journal of Analysis and Applications* (2023), 21:0.
21. M. Ahmad, S. Hussain, I. Zahid, U. parveen, M. Sultan and A. Qayyum, On degree based topological indices of petersen subdivision graph, *European Journal of Mathematical Analysis* 3 (2023)20.
22. R. M. Kashif, M. Ahmad, A. Qayyum, S. S. Supadi, M. J. Hussain, S. Raza, On Degree-Based Topological Indices of Toeplitz Graphs, *Int.J.Anal.* (2023). 21:111.
23. N. Salamat, M. Kamran, S. Ali, M. A. Alam, and R. H. Khan, "Several characterizations on degree-based topological indices for star of david network," *Journal of Mathematics*, vol. 2021.

Muhammad Asif Javed,
Department of Mathematics and Statistics,
University Of Southern Punjab,
Pakistan.
E-mail address: asifaslam033333@gmail.com

and

A. Q. Baig,
Department of Mathematics and Statistics,
University Of Southern Punjab,
Pakistan.
E-mail address: aqbaig1@gmail.com

and

Mukhtar Ahmad,
Faculty of Computer Science and Mathematics,
Universiti Malaysia Terengganu (UMT), Malaysia.
E-mail address: graphtheory1990@gmail.com

and

Roslan Hasni,
Faculty of Mathematics,
Universiti Malaysia Pahang Al-Sultan Abdullah,
Malaysia.
E-mail address: yuhani@umpsa.edu.my

and

Muhammad Kaleem,
Department of Mathematics and Statistics,
University Of Southern Punjab,
Pakistan.
E-mail address: kaleemrana809@gmail.com

and

Ather Qayyum,
Institute of Mathematical Sciences,
Universiti Malaya,
Malaysia.
E-mail address: dratherqayyum@um.edu.my